Talanta 91 (2012) 88–94

Contents lists available at SciVerse ScienceDirect

Talanta

journal homepage: www.elsevier.com/locate/talanta

Fabrication of new single-walled carbon nanotubes microelectrode for electrochemical sensors application

Nguyen Xuan Viet[a,b], Yoshiaki Ukita[a], Miyuki Chikae[a], Yasuhide Ohno[c], Kenzo Maehashi[c], Kazuhiko Matsumoto[c], Pham Hung Viet[d], Yuzuru Takamura[a,*]

[a] School of Materials Science, Japan Advanced Institute of Science and Technology (JAIST), 1-1 Asahidai, Nomi City, Ishikawa 923-1292, Japan
[b] Faculty of Chemistry, Hanoi University of Science, VNU, 19 Le Thanh Tong, Hoan Kiem District, Ha Noi, Viet Nam
[c] The Institute of Scientific and Industrial Research, Osaka University, 8-1 Mihogaoka, Ibaraki, Osaka 567-0047, Japan
[d] Research Center for Environmental Technology and Sustainable Development (CETASD), Hanoi University of Science, VNU, 334 Nguyen Trai, Thank Xuan District, Ha Noi, Viet Nam

ARTICLE INFO

Article history:
Received 31 October 2011
Received in revised form 12 January 2012
Accepted 12 January 2012
Available online 20 January 2012

Keywords:
Single-walled carbon nanotube
Microelectrode
Electrochemical sensors

ABSTRACT

In this paper, we describe two simple different ways to fabricate an array of single-walled carbon nanotubes (SWCNT) microelectrodes from SWCNT network, grown on Si substrate, through micro-fabrication process. Two kinds of material, photoresist – organic compound and sputtered SiO_2, were used as an insulator layer for these arrays of SWCNT microelectrodes. The SWCNT microelectrodes were characterized by scanning electron microscopy (SEM), Raman spectroscopy, and electrochemical measurements. The SWCNT microelectrodes with sputtered SiO_2 as an insulator exhibit some prior advances to these used photoresist layer as insulator such as much stable in harsh condition (high active organic solvents) and high current density (24.94 $\mu A\,mm^{-2}$ compared to 2.69 $\mu A\,mm^{-2}$, respectively). In addition, the well-defined geometry of SWCNT microelectrodes is not only useful for investigating kinetics of electron transfer, but also promising candidate in electrochemical sensors application.

1. Introduction

Carbon nanotubes (CNTs), discovered by Ijima in 1991 [1], is the next generation of carbon materials. They have distinct structural and electronic properties compared to conventional carbon materials that have been widely used in electrochemistry such as glassy carbon (GC), graphite, and carbon fiber [2,3]. The combination of high aspect ratio, nanometer sized dimensions, good electrical conductivity, and low capacitance [4] in the pristine state dictates that CNTs have the capability to make excellent electrode materials [5].

Random networks of single-walled carbon nanotubes (SWCNTs), which lie flat on the insulator support surface, have multiply interconnected points at high density of networks. They have conductive length scales much longer than the individual nanotubes. In fact, they have acting effect like thin conducting film [6]. These SWCNT networks have shown interesting properties for electrical and electrochemical applications [5,6].

There is much attention in using SWCNT to fabricate electrode in the small dimension, because there are several benefits of using small-scale electrodes in electrochemical sensors. Firstly, since current (i) is proportional to the electrode area, small-scale electrodes will further reduce the Ohmic (iR) drop distortion and can be used to detect electrochemical reactions in poorly conducting media, even in the absence of a supporting electrolyte [7]. Secondly, double-layer capacitances are proportional to electrode area. Thus they are greatly reduced for small-scale electrodes which have small surface area, resulting small RC (R: resistance, C: capacitance) time constants in electrochemical cells [8]. Thirdly, the rate of mass transport to and from the electrode (and the related current density) increases as the electrode size decreases [9,10].

Normally, CNT electrodes are prepared essentially by randomly dispersing or confining the CNTs on a conducting substrate, most commonly glassy carbon. This is achieved by drop casting [11], abrasive attachment [12] or directly grown random CNTs network on metal substrates by chemical vapor deposition (CVD) [13,14]. But, in these CNT electrodes, the supporting conductive substrates are not electrically isolated the electrolyte solution, so that the electrochemical signals came from both CNTs and supporting substrate. Thus, they are unsuitable for fundamental electrochemical studies, as it is difficult to quantitatively isolate the SWCNT response from that of the support substrate.

Several techniques have been developed for fabrication of the well-defined geometry microelectrodes based on CNTs, in which the support substrate was isolated, at the range of nano [7,9,15] to micro scale [8,13,14,16]. Koehne et al. fabricated nanoelectrode arrays using vertically aligned multi-walled carbon nanotubes (MWCNT) embedded within SiO_2 matrix. Only the end of MWCNT was protruded to expose to solution by using chemical mechanical

* Corresponding author. Tel.: +81 761 51 1661; fax: +81 761 51 1665.
E-mail address: yztakamura@jaist.ac.jp (Y. Takamura).

0039-9140/$ – see front matter © 2012 Elsevier B.V. All rights reserved.
doi:10.1016/j.talanta.2012.01.023

polishing process [7]. Macpherson et al. fabricated ultramicroelectrodes from SWCNT networks grown on Si wafer through a conventional photolithography process. The photoresist was used as insulator layer [8]. However, the challenges of manipulating a CNTs probe, the contamination and breakdown during fabrication or the unstable of electrode in high active organic solvents [8,9,15] prevent them from wide applications.

In this work, we report the novel approach and simple method to fabricate an array of SWCNT microelectrodes based on SWCNT network through conventional photolithography. These microelectrodes are robust, can be fabricated in high yield, and are of uniform diameter. The SWCNT networks were directly grown on Si substrate using ethanol CVD. Two distinguish insulators, sputtered SiO_2 and photoresist, were used for fabricating of SWCNT microelectrodes. The effects of insulator layers and the ways fabricating insulator layers on the electrochemical properties of SWCNT microelectrodes were investigated. The couple $K_3[Fe(CN)_6]/K_4[Fe(CN)_6]$ was used as a benchmark to characterize the electron transfer properties of SWCNT microelectrodes.

2. Experimental

2.1. Reagent

$Fe(NO_3)_3{\cdot}9H_2O$, $Mo(acac)_2$, KCl, $K_3[Fe(CN)_6]$ were purchased from Wako Pure Chemical Industries (Japan). Other reagents were of analytical grade, and all solutions were prepared and diluted using ultra-pure water (18.2 MΩ cm) from the Millipore Milli-Q system.

2.2. Device fabrication

2.2.1. Electric contact on Si wafer

Platinum contacts, thickness of 30 nm with 10 nm Ti adhesive layers, were thermally evaporated onto the Si substrate through a conventional photolithography process and a plasma sputtering method. The Si substrate is the p-type with 100 nm of thermally intrinsic SiO_2. In order to separate between electrodes, a chromium layer (60 nm of thickness) was also sputtered in the middle of platinum contacts. This layer then was removed off after the catalytic process by chromium etchant solution to leave the blank space of Si wafer between electrodes on the same Si wafer.

2.2.2. Growth of SWCNT network

SWCNT network was grown on Si substrate by ethanol CVD method [17]. The Si substrate was immersed in the catalyst solution consisting of $Fe(NO_3)_3{\cdot}9H_2O$, $Mo(acac)_2$, and alumina nanoparticles for 10 min, and dried in the air for 10 min [18]. The catalyst coated Si substrate was baked at 130 °C in 3 min before transferring into CVD machine. The substrate was heated to 825 °C in CVD machine under argon gas and then argon gas was replaced by ethanol vapor. The growth process was conducted for 10 min.

2.2.3. Apply the insulator layer on SWCNT network

a) SiO_2 layer

The procedure for fabricating SWCNT microelectrodes is shown in Fig. 1a. A chromium layer (200 nm) was, firstly, thermally evaporated onto the SWCNT network using the plasma sputtering method. A photoresist layer with thickness of 15 μm (PMER photoresist) was subsequently spun over the chromium layer. Disk type patterns of 180 μm diameter inside the Pt contacts were formed by exposing to the 458 nm He light for 30 s and developing in PG-7 solution. The exposed chromium layer was removed by chromium etchant solution in 2 min. Then a thermal SiO_2 layer of 250 nm was sputtered on exposed SWCNT network by the plasma sputtering method. Finally, the residue disk type of the photoresist layers and chromium layers were clean by remover and chromium etchant solution, respectively. Note that between two continuous steps, the SWCNT microelectrodes were washed by Mili-Q water for 1 min and then blown under N_2 gas to dry. This SWCNT microelectrode is labeled electrode S.

b) Photoresist layer

The process is depicted in Fig. 1b. According to this way, a photoresist layer of thickness 15 μm was directly spun on surface of SWCNT network via conventional photolithography process. This layer was then exposed to the 458 nm He light in 30 s with mask pattern of disk type microelectrode. The diameter of disk type microelectrode was also 180 μm. Finally the photoresist layer was developed in the PG-7 developing solution and subsequently washed by pure water to get the SWCNT microelectrode. This SWCNT microelectrode is named electrode P.

In both ways, 24 SWCNT microelectrodes were arrayed on a single Si substrate of 25 mm × 30 mm.

2.2.4. Measurement

Scanning electron microscopy (SEM) images were obtained using Hitachi S-4100 with accelerating voltage 20 kV. Raman spectra were performed with laser excitation energy of 514.5 nm on Micro-Raman machine.

Electrochemical measurements were performed on ALS/CH Instruments electrochemical analyzer, model 730C (USA) as shown in Fig. 1c, in which three electrodes system were used with Pt wire as counter, AgCl/Ag micro-electrode as reference (Microelectrodes Inc., USA) and SWCNT microelectrodes as working electrode. A drop of KCl 0.1 M solution (25 μl) containing interested electroactive species was placed in the PDMS chamber over the exposed SWCNT area.

Cyclic voltammetric measurement on as-grown SWCNT network was conducted by using cone capillary cell, in which the top and bottom inner diameter of capillary are 3 mm and 0.5 mm, respectively [19]. The counter and micro-reference electrode were placed inside the capillary. The approach of capillary to the surface of SWCNT network was performed by using the manually controlled x-y-z positioner. By this way, the bottom tip of capillary will not contact with the surface of SWCNT network.

The electrodeposition of Au on SWCNT microelectrodes was conducted by chronoamperometric technique. The constant potential of −0.4 V versus Ag/AgCl was applied on these microelectrodes for a period of 20 s in 0.1 M phosphate buffer saline PBS solution containing 10 mM HAuCl [19].

3. Results and discussion

3.1. Characterization of SWCNT network and microelectrode

The SEM image of as-grown SWCNT network, shown in Fig. 2a, clearly illustrates high density of as-grown SWCNT and they exist in the individual or small bundle tubes. The Raman spectrum of as-grown SWCNT is depicted in Fig. 2b. The shape and position of peaks in Raman spectrum around 1600 cm^{-1} (G band) allow to identify the SWCNT [20]. The characterized peak of disorder graphite at around 1350 cm^{-1} (D band) indicates that there is little amorphous carbon present and that the as-grown SWCNT is high quality, that there are very few defects in SWCNT [17,18,20].

The distribution of SWCNT diameter can be induced from the radial breathing mode (RBM) following equation [20].

$$d = \frac{248}{\lambda} \quad (1)$$

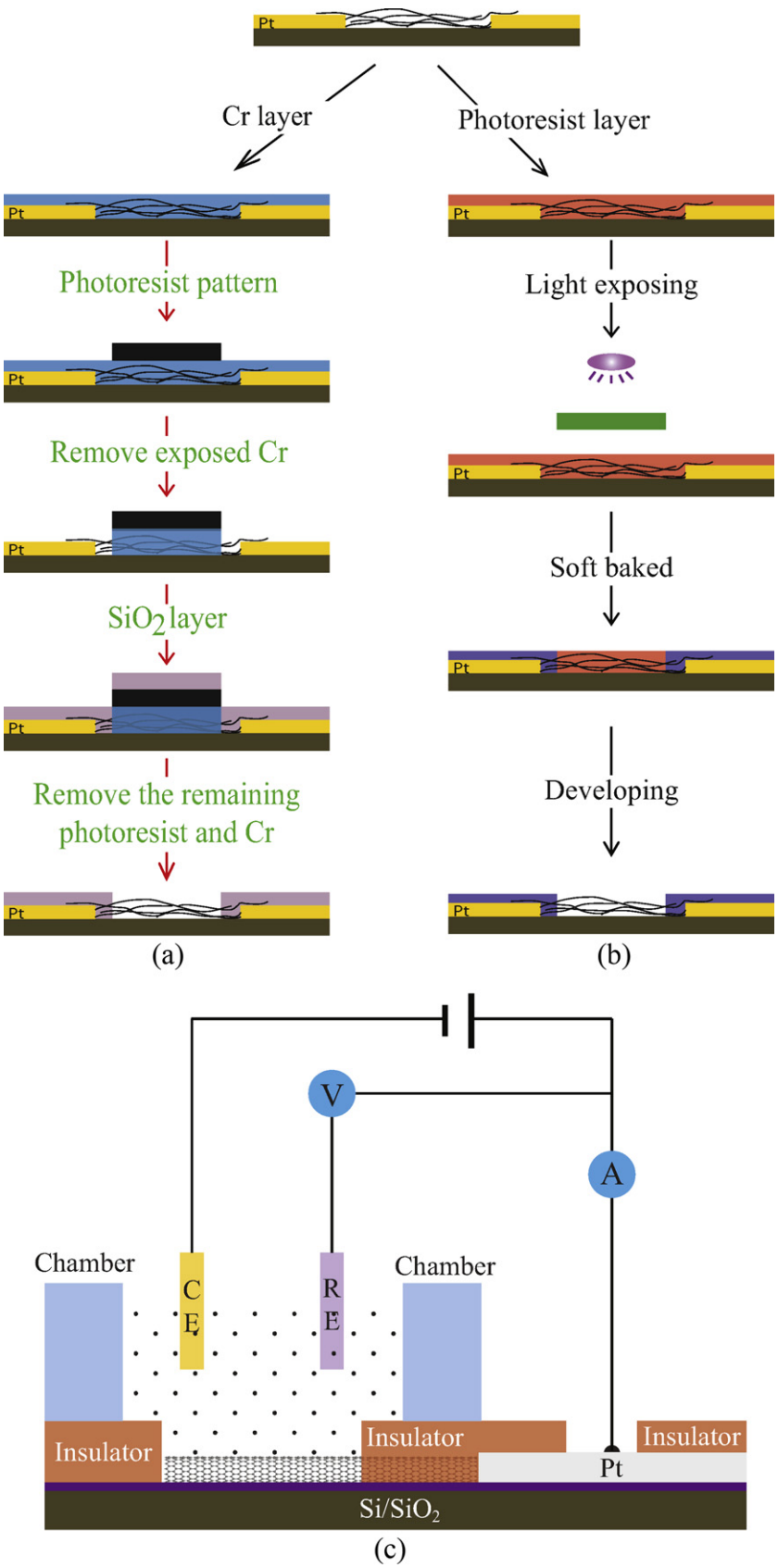

Fig. 1. Schematic of procedure for fabricating SWCNT microelectrodes. (a) Using SiO_2 layer as insulator. (b) Using photoresist layer as insulator. (c) The electrochemical measurement set-up with SWCNT microelectrode as working electrode, Pt wire as counter electrode, and microelectrode Ag/AgCl as reference electrode.

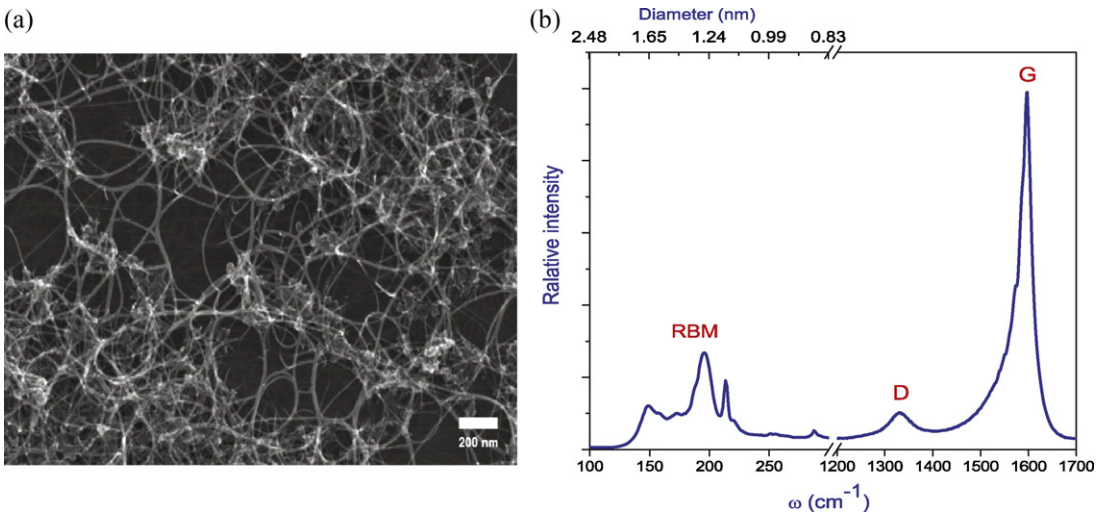

Fig. 2. (a and b) SEM image and Raman scattering spectrum of as-grown SWCNT network, respectively.

where λ is the RBM peak position and d (nm) is the nanotube diameter. From Eq. (1) the nanotube diameter is calculated and given in the upper *x*-axis and the value of nanotube diameter is in range 1.0–2.0 nm, in good agreement with those obtained from published literatures [14,17].

Fig. 3a shows the SEM image of an obtained SWCNT microelectrode. The disk diameter of SWCNT microelectrodes was calculated from the SEM images and got the value of 185 ± 2.6 μm (average of 8 individual samples).

The SEM images of SWCNT network inside electrode S and electrode P are shown in Fig. 3b and c, respectively. The SWCNT networks of electrode P after post treatment processes look slightly thicker than that in as-grown SWCNT network and electrode S as well. The SEM images exhibit that the density of SWCNT networks

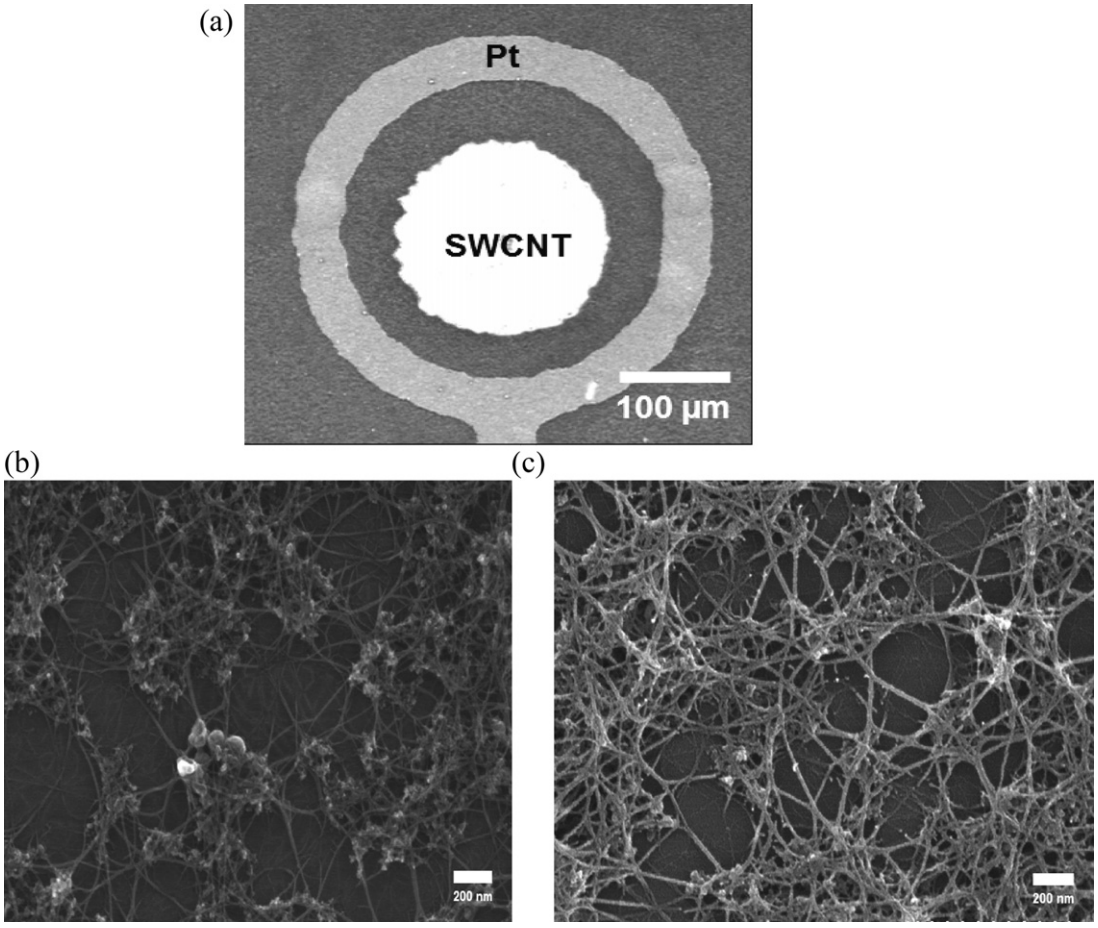

Fig. 3. (a) SEM image of obtained SWCNT microelectrode (b and c) SEM images of SWCNT network inside electrode S and electrode P, respectively.

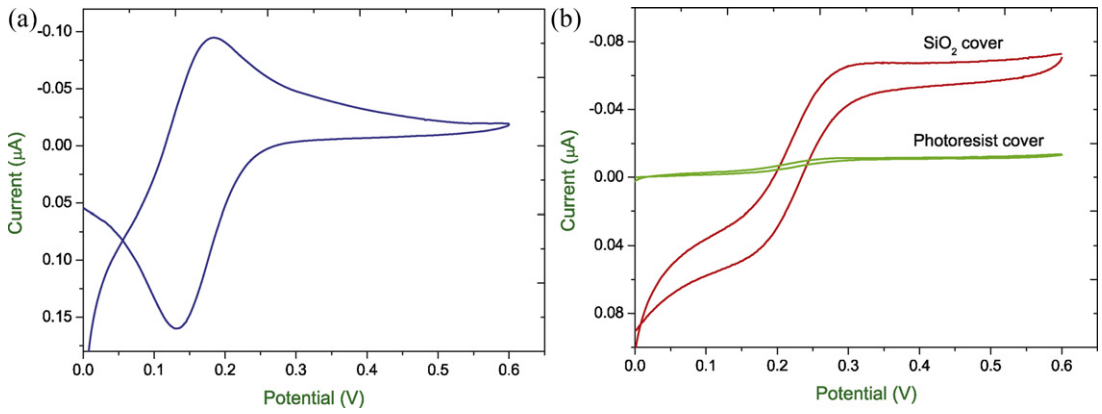

Fig. 4. Cyclic voltammograms in 0.1 M KCl solution containing 0.05 mM $K_3[Fe(CN)_6]/K_4[Fe(CN)_6]$ mixture (1:1 molar ratio) of (a) as-grown SWCNT network (b) electrode S and electrode P. All potential scan rates are 4 mV s^{-1}.

after post processes seem as high as that of as-grown SWCNT (see Fig. 2a). This is because the individual or small bundle of SWCNT entangles each other to increase the stability of network during post processes. In case of electrode S, the surface of SWCNT network was covered entirely by a sputtering Cr layer. The Cr layer, however, finally removed by chromium etchant solution, which specifies to Cr only and does not have any harmful effects to Si substrate and SWCNT network. This Cr layer also acted as a shield to prevent direct contact of organic compounds (photoresist, solvents) to the SWCNT network, which is believed strongly effects on the electrochemical properties of SWCNT [9].

On the other hand, the SiO_2 insulator layer is directly applied on the SWCNT network without the Cr layer. When SiO_2 is removed from SWCNT surface by either wet etching with HF solution [9] or drying etching [14]. Both etching processes could not exactly control removing the upper layer of SiO_2 insulator. One can lead to over etching which break the Si substrate destroying the SWCNT network, another is not completely removed which make SWCNT network inactive at some areas due to the blocking of SiO_2 on the surface of SWCNT (data not shown).

The SiO_2 insulator exhibits some advantages to photoresist insulator [8] including much thermal stable and inert in DMF, DMSO environment. These solvents are usually used as the solvent for linker molecular during the immobilization of antibody on the surface of SWCNT [14,21] in the sensing process compared to photoresist layer.

3.2. Electrochemical properties of the SWCNT microelectrodes

Fig. 4a shows the typical cyclic voltammogram (CV) of as-grown SWCNT electrode in 0.05 mM $K_3[Fe(CN)_6]/K_4[Fe(CN)_6]$ mixture solution (1:1 molar ratio) at potential scan rate 4 mV s^{-1}.

The ΔE_p, peak potential separation of forward and backward curves in a redox couple, is 67 mV suggesting a quasi reversible at the electrode.

For a microelectrode using SWCNT network, the density/separation of individual or small bundle SWCNT is critical [7]. As observed with the high density SWCNT network, the diffusion layers of neighbor individual SWCNT likely overlap. As a result, the CV of this kind of electrodes in measuring the redox species in bulk solution is similar to a solid planar macroelectrode [22].

The high electroactivity of SWCNT has been recently attributed by the present of nano-graphitic "impurity" [23,24], which is rich edge plane material and is the highest electrochemical activity among carbon materials [25–27], in as-grown SWCNT rather than by SWCNT itself.

It is clear that the CNT electrode is driving the electron transfer (ET) reaction faster than many other carbon electrodes surfaces observed [3], with very small apparent activation barrier at the electrode surface.

On the other hand, the SWCNT microelectrodes show the very different CV behavior. Fig. 4b shows typical CVs of two different SWCNT microelectrodes in 0.05 mM $K_3[Fe(CN)_6]/K_4[Fe(CN)_6]$ mixture solution, recorded at a potential scan rate of 4 mV s^{-1}. The CVs show a well-defined sigmoidal shape, characteristic of steady state behavior at ultramicroelectrode (UME). The steady state feature in CV is the strong evidence indicating that most exposed SWCNT behavior as independent nanoelectrode after post grown processes.

The current magnitude at SWCNT electrode S is much high than that of electrode P. The current density is induced from CVs to yield a value of 24.49, and 2.69 μA mm^{-2} for SWCNT electrode S and P, respectively. This illustrates that the electrode S is much electrochemical active than electrode P.

There are some possibilities causing this phenomenon (i) the reduction in density of SWCNT network due to losing of SWCNT in post grown processes (ii) partial blocking surface of SWCNT after the contacting of SWCNT with photoresist, which causes the contamination on SWCNT and (iii) the reduction of nano-graphitic particles in SWCNT network. For electrode S only the reason i and iii can affect to the change of CV characterization.

Because the density of SWCNT networks do not change so much, we tentatively attribute this to the reduction of "impurity" nano-graphitic particles density in SWCNT after post treatment processes. In the case of electrode P, the partial blocking surface of SWCNT by organic compounds from photoresist, which cause the contamination, also affects strongly on the electrochemical properties [9]. In Fig. 5 shows the SEM images of Au electrodeposited on electrode S and P. We confirmed that the white spots in the SEM images are Au by X-ray diffractometry (SEM-EDS) (data not shown). The density of Au particles on electrode S is clearly higher than that on electrode P. This is also the evidence that the electrode S is more active than electrode P.

The current density obtained at electrode S also much high than that of the MWCNT nanoelectrode array [7], SWCNT UME using photoresist as insulator layer [8], and micro carbon fiber electrode [28], 0.4, 2.04 and 9.84 μA mm^{-2}, respectively. The current density at electrode P is slightly higher than that at the UME, which was fabricated using similar method [8].

The hysteresis (shift in half wave potential) between the forward and backward waves indicates a slight departure from a true steady state response, attributed to the partial overlap of diffusion layers at some locations in the randomly distributed network [7].

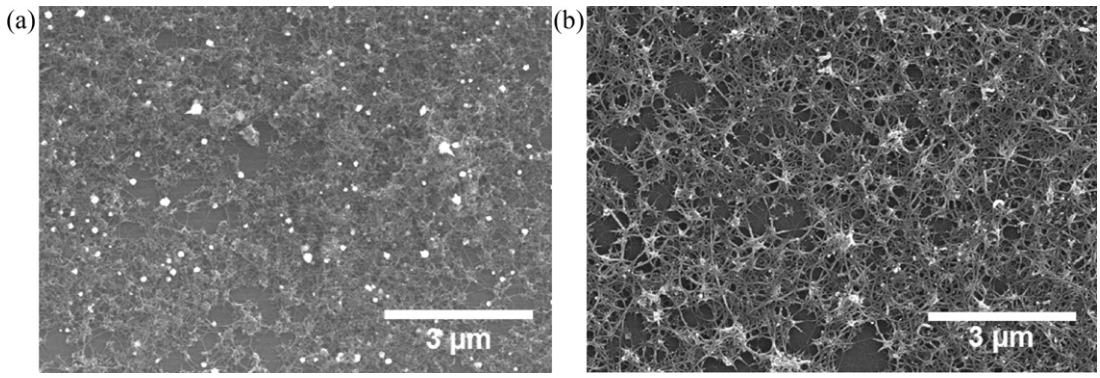

Fig. 5. SEM images of Au particles electrodeposited on (a) electrode S (b) electrode P, respectively.

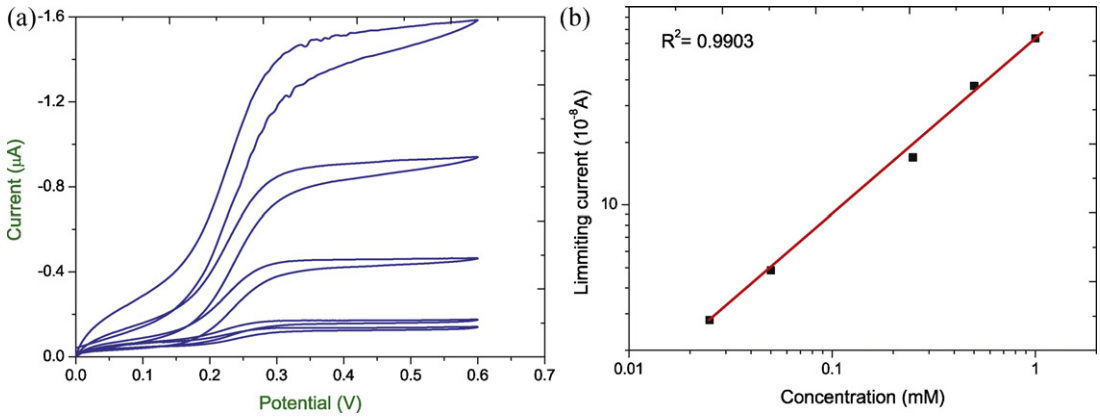

Fig. 6. (a) Cyclic voltammograms of electrode S in 0.1 M KCl solution containing 0.025, 0.05, 0.25, 0.5 and 1.0 mM $K_3[Fe(CN)_6]$]/$K_4[Fe(CN)_6]$ mixture (1:1 molar ratio), scan rate is 4 mV s^{-1}. (b) Plot of limiting currents (at 0.4 V) vs. mediator concentration and linear fit for $K_3[Fe(CN)_6]$.

Fig. 6a shows the CVs of electrode S in the $K_3[Fe(CN)_6]$/$K_4[Fe(CN)_6]$ mixture solution (1:1 molar ratio) in the range of 0.025–1 mM with the potential scan rate of 4 mV s^{-1}.

The diffusion-controlled steady-state limiting current, i_{ss}, at a coplanar disk-shaped microelectrode is given by Eq. (2) [29].

$$i_{ss} = 4nrFDC \quad (2)$$

where n is the number of electrons transferred per redox event, F is the Faraday constant, r is the radius of the disk electrode and C and D are the bulk concentration and diffusion coefficient of the electroactive species, respectively. The use of Eq. (2) is valid because the degree to which the electrode is recessed is minimal compared to its lateral dimension. Fig. 6b shows plot of limiting currents (at 0.4 V) versus redox species concentration. The linear fit through the points indicates a near perfect scaling of i_{ss} with mediator concentration (r^2 is 0.9903). The diffusion coefficient extracted from the slope of the plot is 8.8×10^{-6} cm^2 s^{-1}, which is very good agreement with literature values [29,30].

The observed plateau in cyclic voltammetric response and the scaling of i_{ss} with concentration of redox mediator in the manner predicted by Eq. (2) indicates that the SWCNT microelectrode behaves as a conventional metallic UME (e.g., Pt, Au).

4. Conclusion

We have successfully fabricated the SWCNT microelectrodes based SWCNT network on insulator substrate through microfabrication process. The SWCNT microelectrodes used sputter SiO_2 as insulator exhibit some prior advances to these used photoresist layer as insulator such as much stable in harsh condition (high active organic solvents) and high current density (24.94 compared with 2.69 μA mm^{-2}, respectively). These benefits come from using of Cr layer to cover entirely SWCNT network during the fabricating processes. In addition, the well-defined geometry of SWCNT microelectrodes is not only useful for investigating kinetics electron transfer, but also promising candidate in electrochemical sensors application.

Acknowledgement

This work was partially supported by a Grant-in-Aid for Scientific Research on Priority Areas (No. 19054011) and the Cooperative Research Program of "Network Joint Research Center for Materials and Devices" from the Ministry of Education, Culture, Sports, Science and Technology of Japan.

References

[1] S. Iijima, Nature 354 (1991) 56–58.
[2] A.V. Melechko, V.I. Merkulov, T.E. McKnight, M.A. Guillorn, K.L. Klein, D.H. Lowndes, M.L. Simpson, J. Appl. Phys. 97 (2005) 041301.
[3] R.L. McCreery, Chem. Rev. 108 (2008) 2646–2687.
[4] S. Rosenblatt, Y. Yaish, J. Park, J. Gore, V. Sazonova, P.L. McEuen, Nano Lett. 2 (2002) 869–872.
[5] J. Edgeworth, N. Wilson, J.V. Macpherson, Small 3 (2007) 860–870.
[6] E.S. Snow, P.M. Campbell, M.G. Ancona, J.P. Novak, Appl. Phys. Lett. 86 (2005) 033105.
[7] J. Koehne, J. Li, A.M. Cassell, H. Chen, Q. Ye, H.T. Ng, J. Han, M. Meyyappan, J. Mater. Chem. 14 (2004) 676–684.
[8] I. Dumitrescu, P.R. Unwin, N.R. Wilson, J.V. Macpherson, Anal. Chem. 80 (2008) 3598–3605.
[9] I. Heller, J. Kong, H.A. Heering, K.A. Williams, S.G. Lemay, C. Dekker, Nano Lett. 5 (2005) 137–142.
[10] D. Wei, M.J.A. Bailey, P. Andrew, T. Ryhanen, Lab Chip 9 (2009) 2123–2131.
[11] H. Luo, Z. Shi, N. Li, Z. Gu, Q. Zhuang, Anal. Chem. 73 (2001) 915–920.

[12] C.E. Banks, R.R. Moore, T.J. Davies, R.G. Compton, Chem. Commun. (2004) 1804–1805.
[13] J. Okuno, K. Maehashi, K. Matsumoto, K. Kerman, Y. Takamura, E. Tamiya, Electrochem. Commun. 9 (2007) 13–18.
[14] J. Okuno, K. Maehashi, K. Kerman, Y. Takamura, K. Matsumoto, E. Tamiya, Biosens. Bioelectron. 22 (2007) 2377–2381.
[15] J.K. Campbell, L. Sun, R.M. Crooks, J. Am. Chem. Soc. 121 (1999) 3779–3780.
[16] J.M. Nugent, K.S.V. Santhanam, A. Rubio, P.M. Ajayan, Nano Lett. 1 (2001) 87–91.
[17] K. Maehashi, Y. Ohno, K. Inoue, K. Matsumoto, Appl. Phys. Lett. 85 (2004) 858.
[18] H.E. Unalan, M. Chhowalla, Nanotechnology 16 (2005) 2153–2163.
[19] P.V. Dudin, P.R. Unwin, J.V. Macpherson, J. Phys. Chem. C 114 (2010) 13241–13248.
[20] M.S. Dresselhaus, G. Dresselhaus, A. Jorio, A.G. Souza Filho, M.A. Pimenta, R. Saito, Acc. Chem. Res. 35 (2002) 1070–1078.
[21] R.J. Chen, Y. Zhang, D. Wang, H. Dai, J. Am. Chem. Soc. 123 (2001) 3838–3839.
[22] J. Li, A. Cassell, L. Delzeit, J. Han, M. Meyyappan, J. Phys. Chem. B 106 (2002) 9299–9305.
[23] M.E. Itkis, D.E. Perea, R. Jung, S. Niyogi, R.C. Haddon, J. Am. Chem. Soc. 127 (2005) 3439–3448.
[24] P.-X. Hou, C. Liu, H.-M. Cheng, Carbon 46 (2008) 2003–2025.
[25] C.E. Banks, R.G. Compton, Analyst 131 (2006) 15–21.
[26] M. Pumera, Chem. Eur. J. 15 (2009) 4970–4978.
[27] A. Ambrosi, M. Pumera, Chem. Eur. J. 16 (2010) 10946–10949.
[28] Micro carbon fiber electrode (BAS Inc., Japan), diameter: 33 μm.
[29] L.R.F. Allen, J. Bard, Electrochemical Methods: Fundamentals and Applications, 2nd ed., 2001.
[30] J.L. Conyers, H.S. White, Anal. Chem. 72 (2000) 4441–4446.